Resilient Leader-Follower Formation Control for Nonholonomic Systems Using Channel State Feedback

Bin Hu and M.D. Lemmon

***Abstract*— Leader-follower formation control is a widely used control strategy that often needs systems to exchange information over a wireless radio communication network. These wireless networks are subject to *deep fades*, where a severe drop in the quality of the communication link occurs. Such deep fades may significantly impact the formation's performance and stability. In many applications, however, the variation in channel state is a function of the system's kinematic states. This suggests that one can use channel state information as a feedback signal to recover the performance loss caused by a deep fade. This paper derives sufficient conditions to assure almost-sure asymptotic stability of a leader-follower nonholonomic system in the presence of deep fades. These conditions relate the channel state to the system's convergence rate. This paper uses this fact to reconfigure the controller. Simulation results are used to illustrate the main results in the paper.**

I. Introduction

In the past decade, *formation control* has found extensive applications in industry and academia [2], [14], [11], [13], [5]. In formation control, the agents coordinate with each other to form and maintain a specified formation. The coordination is often conducted over a wireless radio communication network. It is well known that such communication networks are subject to deep fading, which causes a severe drop in the network's quality-of-service (QoS). These deep fades negatively impact the formation's performance and stability by interfering with the coordination between agents. The loss of coordination may cause serious safety issues in applications like smart transportation system [19], unmanned aerial vehicles system[16] and underwater autonomous vehicles[15]. These issues can be addressed by developing a resilient control system that detect such deep fades and adaptively reconfigures its controller to maintain a minimum performance level.

Channel fading is often characterized in terms of channel gain [18]. Channel gain represents the signal strength ratio of receiving signal over transmission signal. It is usually modeled as an *independent and identical distributed (i.i.d)* random process with Rayleigh or Rician distribution. This model is inadequate in two aspects. First, the fading process exhibits memory which is better modeled as a Markov random process with two states [20]. Second, the i.i.d. channel model is ignores the impact that the formation's kinematic states have on the channel. Vehicle-to-Vehicle (V2V)[4] systems provide an example in which the velocity and relative distance of the vehicles significantly affect the channel state. Moreover, for those wireless communication systems using directional antennae [23], [1], changes in the relative vehicle orientation could also lead to a deep fade.

The loss of information caused by deep fades negatively limits the performance that can be achieved by the control system. Prior work [21], [17], [6] characterized the minimum stabilizing bit rate for linear time-invariant system assuming constant channel gain. As noted above, the assumption on constant channel gain is overly simplistic for fading channels. An initial attempt to study the impact of the time-varying channel gains on mean square stability appeared in [12]. This work, however, assumed the channel gain was functionally independent from the physical system's dynamics. In [8], the authors examined a more realistic fading channel model in which the channel is exponentially bursty and is dependent on the norm of the physical system's states. This paper extends the prior work in [8] to a two-dimensional leader-follower formation control problem.

Leader-follower formations are useful for their simplicity and scalability. This paper studies the leader-follower control scheme for nonholomonic systems using directional antennae to access the wireless communication network. Assuming an exponentially bursty channel model, this paper derives conditions that are sufficient for the system to have *almost-sure stability* [9]. The paper uses this characterization to propose adaptive control schemes that switch feedback controllers in response to changes in channel state. The simulation results demonstrate the merits of the proposed method.

II. Mathematical Preliminaries

Let $\mathbb{Z}$ and $\mathbb{R}$ denote the set of integers and real numbers, respectively. Let $\mathbb{Z}_+$ and $\mathbb{R}_+$ denote the set of positive integers and non-negative real numbers, respectively. Let $\mathbb{R}^n$ denote the n-dimensional Euclidean vector space. Consider a continuous-time random process $\{x(t) \in \mathbb{R}^n : t \in \mathbb{R}_+\}$ whose sample paths are right-continuous and satisfy the following differential equation,

$$\dot{x}(t) = f(x(t), u(t), w(t)) \tag{1}$$

where $f(0,0,0) = 0$, $u(\cdot) : \mathbb{R}_+ \to \mathbb{R}^m$ is a control input and $w(t)$ is a jump process

$$w(t) = \sum_{\ell=1}^{\infty} w_\ell \delta(t - \tau_\ell) \tag{2}$$

in which $\{w_\ell, \ell \in \mathbb{Z}_+\}$ is a Markov process describing the ℓth jump's size at jump instants $\{\tau_\ell\}_{\ell=1}^{\infty}$. The expectation of this stochastic process at time t will be denoted as $\mathbb{E}(x(t))$.

The authors are with Department of Electrical Engineering, University of Notre Dame, Notre Dame, IN 46556, USA. bhu2,lemmon@nd.edu.
The authors gratefully acknowledge the partial financial support of the National Science Foundation (CNS-1239222)

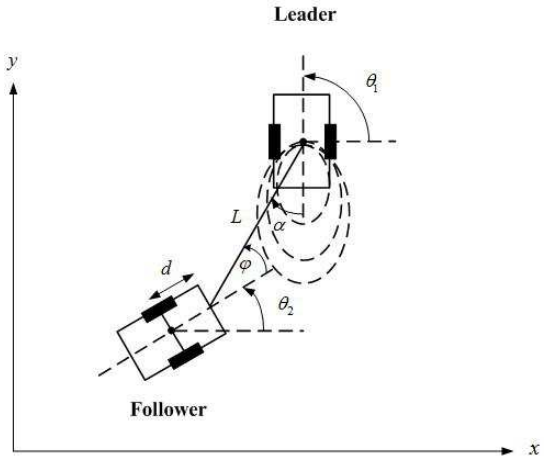

Fig. 1. The leader-follower formation

The system in equations (1-2) is said to be *almost-surely* asymptotically stable if for all $\varepsilon > 0$ and $\rho > 0$, there exists $T > 0$ and $\delta > 0$ such that if $|x(0)| \leq \delta$, then

$$\Pr\left\{\sup_{t \geq T} |x(t)| \geq \varepsilon\right\} \leq \rho$$

Any stochastic process that satisfies the above condition will be said to be almost-surely convergent. A discrete-time Markov process $\{U_k \in \mathbb{R} : k \in \mathbb{Z}_+\}$ will be said to be a *supermartingale* if and only if

$$\mathbb{E}(U_k | U_{k-1}) \leq U_{k-1}$$

for all $k \in \mathbb{Z}_+$. If $\{U_k\}$ is a supermartingale, then one can use the Markov inequality to infer that this process is also almost-surely convergent.

III. System Model

Figure 1 shows the leader-follower system's geometry. The ith vehicle's position ($i = 1,2$) at time $t \in \mathbb{R}_+$ is denoted by the ordered pair $(x_i(t), y_i(t))$. The attitude of the vehicle relative to the $y = 0$ axis at time t is denoted as $\theta_i(t)$. The position and attitude trajectories satisfy the differential equations

$$\dot{x}_i = v_i \cos(\theta_i), \dot{y}_i = v_i \sin(\theta_i), \dot{\theta}_i = \omega_i \tag{3}$$

where the control inputs, v_i and ω_i, are the vehicle's speed and angular velocity, respectively. Throughout this paper vehicle 1 is the leader and vehicle 2 is the follower. The leader can directly measure its bearing angle, α, relative to the follower. Similarly, the follower can measure its bearing angle, ϕ, relative to the leader. Both vehicle's can measure the distance, L between the vehicles. In the following, it will be convenient to characterize the time rate of change of the the relative distance, L, and leader's relative bearing, α

$$\begin{aligned} \dot{L} &= v_1 \cos\alpha - v_2 \cos\phi - d\omega_2 \sin\phi \\ \dot{\alpha} &= \tfrac{1}{L}(-v_1 \sin\alpha + v_2 \sin\phi + d\omega_2 \cos\phi) + \omega_1 \end{aligned} \tag{4}$$

The control objective is to have the follower adjust its velocity, v_2 and angular rate ω_2, to achieve and maintain a desired inter-vehicle distance, L_d, and relative bearing angle, α_d. We assume that the leader does not change its speed, v_1, but it regulates its angular velocity $\omega_1 = g(\alpha)$ as a function of its relative bearing, α. The functional form of $g(\cdot)$ is known to the follower. What is not directly known by the follower is the leader's relative bearing angle, α. This measurement must be transmitted from the leader to the follower over a wireless channel that is accessed using a directional antenna whose radiation pattern is shown in Figure 1.

The leader samples and quantizes its measurement of the bearing angle, α, before transmitting this measurement to the follower. A sequence $\{\tau_k\}_{k=1}^{\infty}$ characterizes the sampling instants with $\tau_k < \tau_{k+1}$ for $k = 1,2,\ldots,\infty$. The kth sampled measurement is quantized with $\overline{R}$ bits over the interval $[\overline{\alpha}_k - U_k, \overline{\alpha}_k + U_k]$. The ordered pair $(\overline{\alpha}_k, U_k)$ represent the "state" of the quantizer at the kth time instant with $\overline{\alpha}_k$ representing the "center" of an *uncertainty interval* and U_k representing the length of that interval. It is assumed that the sequence $\{\overline{\alpha}_k, U_k\}_{k=1}^{\infty}$ is known to both leader and follower. We let $c_k = \{b_{ik}\}_{i=1}^{\overline{R}}$ denote the kth *codeword* transmitted by the leader. This kth codeword consists of bits $b_{ik} \in \{-1,1\}$ for $i = 1,2,\ldots,\overline{R}$ that satisfy the following equation

$$\alpha(\tau_k) = \overline{\alpha}_k + U_k \sum_{j=1}^{\overline{R}} \frac{1}{2^j} b_{jk}$$

This corresponds to a uniform quantization of the sampled state within the interval $[\overline{\alpha}_k - U_k, \overline{\alpha}_k + U_k]$.

The codeword, c_k, is transmitted over an unreliable wireless channel, so that only the first R_k bits are received at the decoder by time $a_k = \tau_k + \Delta$. We refer to a_k as the arrival time. Δ represents a *deadline* after which the receiver stop listening for the the leader's transmission and uses the bits it has received to reconstruct the leader's bearing angle. Under this model, the follower's estimate of the leader's transmitted bearing angle takes the form,

$$\hat{\alpha}_k = \overline{\alpha}_k + U_k \sum_{j=1}^{R_k} \frac{1}{2^j} b_{jk}$$

The follower then uses the estimated bearing angle, $\hat{\alpha}_k$, and the measured inter-vehicle distance, L, to select its speed, v_2, and angular speed, ω_2, to achieve the control objectives.

The number of received bits, $\{R_k\}_{k=1}^{\infty}$ is a random process exhibiting *exponentially bounded burstiness*. Let $r_k = \frac{R_k}{\Delta}$ denote the instantaneous bit-rate at the kth transmission. Let $h(\cdot,\cdot)$ and $\gamma(\cdot,\cdot)$ denote continuous, positive and monotone decreasing functions from $\mathbb{R} \times \mathbb{R}_+$ to $\mathbb{R}_+$. The probability for R_k is assumed to satisfy

$$\Pr\{R_k \leq h(\alpha(\tau_k), L(\tau_k)) - \sigma\} \leq e^{-\gamma(\alpha(\tau_k), L(\tau_k))\sigma} \tag{5}$$

for $|\alpha| \leq \pi/2$ and $\sigma \in [0, h(\alpha(\tau_k), L(\tau_k))]$. The function $h(\alpha, L)$ may be seen as a threshold characterizing the low bit-rate region as a function of the formation's current state. The bound in (5) says that the likelihood of having low bit-rates is an exponentially decreasing function of how far away one is from that low bit-rate region. The exponent associated with that exponential decrease is represented by the function

$\gamma(\alpha, L)$. What should be apparent in this model is that we are explicitly accounting for the relationship between channel state and formation configuration. A major goal of this paper is to exploit that relationship in deciding how to switch between different controllers.

In this paper, the follower switches among a group of controllers to regulate the inter-vehicle distance, L, and bearing angle α. The objective is to steer the system to a desired distance, L_d, and bearing angle, α_d, and then maintain that setpoint. At time $a_k = \tau_k + \Delta$, the follower receives the leader's measurement of its bearing angle $\alpha(\tau_k)$ and then reconstructs an estimate of that measurement which we denote as $\hat{\alpha}_k$. The control gains at time instant k are $(k_\alpha(k), k_L(k))$. These gains are selected from one pair of a collection of values $\mathscr{K} = \{K_1, K_2, \ldots, K_N\}$, where $K_i = \{(k_{\alpha i}, k_{Li}) | k_{\alpha i}, k_{Li} \in \mathbb{R}_+\}$. We make use of a standard feedback linearization method to generate the control inputs

$$\begin{aligned} v_2 &= \frac{v_1 \cos\tilde{\alpha} + d\omega_2 \sin\phi - k_L(k)(L - L_d)}{\cos\phi} = K_v(L, \tilde{\alpha}_k) \\ \omega_2 &= \frac{\cos\phi}{d}[Lk_\alpha(k)(\alpha_d - \tilde{\alpha}) - Lg(\tilde{\alpha}) + v_1 \sin\tilde{\alpha} \\ &\quad + k_L(k)\tan\phi(L - L_d) - v_1 \tan\phi\cos\tilde{\alpha}] = K_\omega(L, \tilde{\alpha}) \end{aligned}$$

over the interval $[a_k, a_{k+1}]$. The variable $\tilde{\alpha}$ is a continuous function of time representing the follower's prediction of the bearing angle over the time interval $[a_k, a_{k+1}]$. This prediction satisfies the following initial value problem for $t \in [a_k, a_{k+1}]$

$$\dot{\tilde{\alpha}} = k_\alpha(k)(\alpha_d - \tilde{\alpha}), \quad \tilde{\alpha}(a_k) = (\hat{a}_k - \alpha_d)e^{-k_\alpha(k-1)\Delta} + \alpha_d \quad (6)$$

With this control, the inter-vehicle distance, L, and leader bearing angle α satisfy the following differential equation over $[a_k, a_{k+1}]$.

$$\dot{L} = k_L(k)(L_d - L) + v_1(\cos\alpha - \cos\tilde{\alpha}) \quad (7)$$

$$\dot{\alpha} = \frac{v_1}{L}(\sin\tilde{\alpha} - \sin\alpha) + k_\alpha(k)(\alpha_d - \tilde{\alpha}) + g(\alpha) - g(\tilde{\alpha}) \quad (8)$$

for all $k = 1, 2, \ldots, \infty$. Equations (6-8) represent the closed-loop state equations for this system with input v_1. These system equations actually form a jump process of form given in equations (1-2) where the jumps occur at discrete times $\{a_k\}_{k=1}^{\infty}$ with a magnitude $\hat{\alpha}_k$ whose random nature is driven by the number of received bits R_k.

Remark 3.1: The characterization of geometric changes on inter-vehicle distance L and bearing angle α in equation (4) is widely used in the literature. The pioneering work on this model can be found in [5].

Remark 3.2: The probability bound in equation (5) can be viewed as a slight modification of the traditional *exponential bounded burstiness* (EBB) model [22]. The only difference lies in our characterization of the system state's impact on the model. Traditional i.i.d. channel models are EBB, but two-state Markov chains also satisfy an EBB bound. In this regard, our use of the exponentially bursty channel model can be applied to more realistic channels. In addition to this, the probabilistic nature of the bound fits well with the definition of almost-sure stability, thereby allowing us to establish results for a much stronger notion of stability than mean-square stability.

Remark 3.3: The quantization method adopted in this paper is similar to the well known dynamic quantization approach in [17], [3], [10]. Traditionally, dynamic quantization is used to achieve asymptotic stability for the deterministic system. In this paper, this approach is applied to achieve almost-sure asymptotic stability.

Remark 3.4: The use of switching controllers to adjust for changes in system structure has been investigated in [7]. The novelty in this paper is its use of that idea to reconfigure in response to changes in channel state.

IV. Main Results

The paper's main result consists of two parts regarding the behavior of the functions $\alpha(t)$ and $L(t)$ satisfying equations (6-8). The first part provides sufficient conditions under which the relative distance, $L(t)$, is convergent to a compact invariant interval. The second part provides sufficient conditions for the almost-sure asymptotic stability of the bearing angle, $\alpha(t)$.

A. Convergence of Inter-vehicle Distance, L

The following lemma provides a sufficient condition on the gain k_L, under which one can show $L(t)$ converges at an exponential rate to an invariant set Ω_{inv} centered at the desired inter-vehicle distance L_d.

Lemma 4.1: Consider the system (6-8) with the controller gain pair $(k_\alpha, k_L) \in \mathscr{K}$. If $k_L > \frac{2v_1}{\delta(L_d - d)}$ and $L(0) > d$, then for any sample path, $L(t) \geq d$ for all $t \in \mathbb{R}_+$ and there exists a finite time $\overline{T} > 0$ such that $L(t)$ enters and remains in the set

$$\Omega_{\text{inv}} \equiv \left\{ L \in \mathbb{R}_+ \,|\, |L - L_d| \leq \frac{2v_1}{\delta k_L} \right\}$$

for all $t \geq \overline{T}$ and any $\delta \in (0, 1]$.

Proof: Consider the function $V(L) = \frac{1}{2}(L - L_d)^2$. Taking the directional derivative of V, one obtains

$$\begin{aligned} \dot{V}(L) &= -k_L(L - L_d)^2 + (L - L_d) \cdot v_1(\cos\alpha - \cos\overline{\alpha}) \\ &\leq -k_L(1 - \delta)(L - L_d)^2 - \delta \cdot k_L(L - L_d)^2 \\ &\quad + 2|L - L_d| v_1 \end{aligned}$$

for any $\delta \in (0, 1]$. The last inequality holds because $|\cos\alpha - \cos\overline{\alpha}| \leq 2$. When $|L - L_d| \geq \frac{2v_1}{\delta k_L}$, the following dissipative inequality holds,

$$\dot{V}(L) \leq -k_L(1 - \delta)(L - L_d)^2 = -2k_L(1 - \delta)V(L) \quad (9)$$

This is sufficient to imply that $V(L(t))$ is an exponentially decreasing function of time that enters the set Ω_{inv} in finite time. $L(t) \geq d$ for all time since all L in Ω_{inv} satisfy

$$d < \frac{2v_1}{\delta k_L} - L_d \leq L \leq \frac{2v_1}{\delta k_L} + L_d \quad (10)$$

■

The following corollary characterizes lower and upper bounds on the relative distance trajectory $L(t)$. These characterizations are used later Lemmas 4.3 and 4.6.

Corollary 4.2: Under the assumptions of Lemma 4.1, the inter-vehicle distance $L(t)$ for $t \geq t_0$ can be bounded as

$$L(t) \leq [L(t_0) - (L_d + \frac{2v_1}{k_L})]e^{-k_L(t-t_0)} + (L_d + \frac{2v_1}{k_L}) \quad (11)$$

$$L(t) \geq [L(t_0) - (L_d - \frac{2v_1}{k_L})]e^{-k_L(t-t_0)} + (L_d - \frac{2v_1}{k_L}) \quad (12)$$

Proof: From equation (7), we have

$$\begin{aligned} \dot{L} &\leq k_L(L_d - L) + 2v_1 \\ \dot{L} &\geq k_L(L_d - L) - 2v_1 \end{aligned}$$

Using Gronwall-Bellman inequality over the time interval $[t_0, t]$, the final result is obtained. ■

B. Almost-sure Asymptotic Stability for Bearing Angle α

The sequence $\{\overline{\alpha}_k, U_k\}_{k=0}^{\infty}$ characterizes the quantizer's state at each time instance τ_k. The following lemma gives a recursive construction for this sequence such that the quantization error, $|\alpha(\tau_k) - \hat{\alpha}(\tau_k)|$ remains bounded for all $k \geq 0$.

Lemma 4.3: Given the sequences $\{\tau_k\}_{k=0}^{\infty}$, $\{a_k\}_{k=0}^{\infty}$ and $\{k_\alpha(k), k_L(k)\}_{k=0}^{\infty}$, let $T = \tau_{k+1} - \tau_k$ and $\Delta = a_k - \tau_k$. Suppose the initial ordered pair $(\overline{\alpha}_0, U_0)$ and controller gain $(k_L(0), k_\alpha(0))$ are known to both leader and follower, the initial system state $\alpha(0) \in [-U_0, U_0]$, $|U_0| \leq \frac{\pi}{2}$, and the function $g(\cdot) : \mathbb{R} \to \mathbb{R}$ in equation (8) is locally Lipschitz with Lipschitz constant $\bar{L}$. If the sequence $\{\overline{\alpha}_k, U_k\}_{k=0}^{\infty}$ is constructed by the following recursive equation,

$$\begin{aligned} U_{k+1} &= 2^{-R_k}\Lambda_k(k_L(k-1), k_L(k))U_k, \forall k \geq 0 \quad (13) \\ \overline{\alpha}_{k+1} &= (\hat{\alpha}_k - \alpha_d)e^{-k_\alpha(k-1)\Delta - k_\alpha(k)(T-\Delta)} + \alpha_d \quad (14) \end{aligned}$$

where $\Lambda_k = \Lambda_{1,k}(k_L(k-1))\Lambda_{2,k}(k_L(k))$ satisfies

$$\begin{aligned} \Lambda_{1,k} &= (\frac{L(\tau_k)}{(L(\tau_k) - L_{M,k-1})e^{-k_L(k-1)\Delta} + L_{M,k-1}})^{M_{1,k}} e^{\bar{L}\Delta} \\ \Lambda_{2,k} &= (\frac{L(a_k)}{(L(a_k) - L_{M,k})e^{-k_L(k)(T-\Delta)} + L_{M,k}})^{M_{2,k}} e^{\bar{L}(T-\Delta)} \\ M_{1,k} &= \frac{v_1}{k_L(k-1)(L(\tau_k) - L_{M,k-1})} \\ M_{2,k} &= \frac{v_1}{k_L(k)(L(a_k) - L_{M,k})} \\ L_{M,k-1} &= L_d - \frac{2v_1}{k_L(k-1)} \end{aligned}$$

then the quantization error in the bearing state generated by system equations (6-8) can be bounded as

$$|\alpha(\tau_k) - \hat{\alpha}(\tau_k)| \leq \bar{U}_k, \forall k \geq 0. \quad (15)$$

where $\bar{U}_k = 2^{-R_k}U_k$ and R_k is the number of bits received over the time interval $[\tau_k, a_k)$.

Proof: Let $e_k(t) = \alpha(t) - \tilde{\alpha}(t)$ denote the estimation error over the time interval $[\tau_k, \tau_{k+1}]$, we know that the system state α and the prediction $\tilde{\alpha}$ satisfy,

$$\begin{aligned} \dot{\alpha} &= \frac{v_1}{L}(\sin\tilde{\alpha} - \sin\alpha) + k_\alpha(\alpha_d - \tilde{\alpha}) + g(\alpha) - g(\tilde{\alpha}), \\ \dot{\tilde{\alpha}} &= k_\alpha(\alpha_d - \tilde{\alpha}) \end{aligned}$$

with $k_\alpha = k_\alpha(k-1)$ at interval $[\tau_k, a_k)$ and $k_\alpha(k)$ at $[a_k, \tau_{k+1}]$. The error dynamics for $\dot{e}_k$, therefore, satisfy,

$$\dot{e}_k = \frac{v_1}{L}(\sin\tilde{\alpha} - \sin\alpha) + g(\alpha) - g(\tilde{\alpha}), t \in [\tau_k, \tau_{k+1}] \quad (16)$$

With $\frac{d|e_k|}{dt} \leq |\dot{e}_k|$, we have

$$\begin{aligned} \frac{d|e_k|}{dt} &\leq \left|\frac{v_1}{L}(\sin\tilde{\alpha} - \sin\alpha) + g(\alpha) - g(\tilde{\alpha})\right| \\ &\leq \left(\frac{v_1}{|L|} + \bar{L}\right)|e_k| \quad (17) \end{aligned}$$

The second inequality holds because $|\sin\tilde{\alpha} - \sin\alpha| \leq |\alpha - \tilde{\alpha}|$ and the local Lipschitz assumption on function $g(\cdot)$.

Consider the time interval $[\tau_k, a_k)$, the inequality (17) is further bounded as

$$\frac{d|e_k|}{dt} \leq \left(\frac{v_1}{(L(\tau_k) - L_{M,k-1})e^{-k_L(k-1)(t-\tau_k)} + L_{M,k-1}} + \bar{L}\right)|e_k| \quad (18)$$

where $L_{M,k-1} = L_d - \frac{2v_1}{k_L(k-1)}$. The inequality holds because of Corollary 4.2. Applying Gronwall-Bellman inequality theorem over $[\tau_k, a_k)$ leads to

$$\begin{aligned} \Lambda_{1,k} &= \left(\frac{L(\tau_k)}{(L(\tau_k) - L_{M,k-1})e^{-k_L(k-1)\Delta} + L_{M,k-1}}\right)^{M_{1,k}} e^{\bar{L}\Delta} \\ |e_k(a_k)| &\leq \Lambda_{1,k}|e(\tau_k)| \end{aligned}$$

where $M_{1,k} = \frac{v_1}{k_L(k-1)(L(\tau_k) - L_{M,k-1})}$. Similarly, consider time interval $[a_k, \tau_{k+1}]$, one can also obtain

$$\begin{aligned} \Lambda_{2,k} &= \left(\frac{L(a_k)}{(L(a_k) - L_{M,k})e^{-k_L(k)(T-\Delta)} + L_{M,k}}\right)^{M_{2,k}} e^{\bar{L}(T-\Delta)} \\ |e_k^-(\tau_{k+1})| &\leq \Lambda_{2,k}|e(a_k)| \end{aligned}$$

where $M_{2,k} = \frac{v_1}{k_L(k)(L(a_k) - L_{M,k})}$ and $e_k^-(\tau_{k+1})$ represents the quantization error at time τ_{k+1} prior to receiving new information, R_{k+1}. Then, the following inequality holds,

$$\begin{aligned} |e_k^-(\tau_{k+1})| &\leq \Lambda_{1,k}\Lambda_{2,k}|e(\tau_k)| \\ &= \Lambda_k(k_L(k-1), k_L(k))|e(\tau_k)| \end{aligned}$$

Assume $|\alpha(\tau_k) - \hat{\alpha}(\tau_k)| \leq \bar{U}_k$ holds, then at time τ_{k+1}, we have

$$\begin{aligned} |e_k^-(\tau_{k+1})| &\leq \Lambda_k(k_L(k-1), k_L(k))|e(\tau_k)| \\ &\leq \Lambda_k(k_L(k-1), k_L(k))\bar{U}_k. \end{aligned}$$

Since there are R_{k+1} bits received over the time interval $[\tau_{k+1}, a_{k+1})$, the uncertainty on state $\alpha(\tau_{k+1})$ is reduced to $\Lambda_k(k_L(k-1), k_L(k))\bar{U}_k 2^{-R_{k+1}}$. Let $\bar{U}_{k+1} = \Lambda_k(k_L(k-1), k_L(k))\bar{U}_k 2^{-R_{k+1}}$, which is equivalent to $U_{k+1} = 2^{-R_k}\Lambda_k(k_L(k))U_k$, the quantization error at $k+1$th transmission time is bounded by $\bar{U}_{k+1}$, i.e. $|e(\tau_{k+1})| \leq \bar{U}_{k+1}$. Since k is arbitrarily chosen for the proof, the result holds for all $k \geq 0$.

The center of the quantizer is reset to $\hat{\alpha}_k$ when R_k bits are received at time a_k, and evolves according to the following two ODEs over time interval $[\tau_k, \tau_{k+1}]$

$$\dot{\overline{\alpha}} = k_\alpha(k-1)(\alpha_d - \overline{\alpha}), t \in [\tau_k, a_k)$$

with initial value $\overline{\alpha}(\tau_k) = \hat{\alpha}_k$, and

$$\dot{\overline{\alpha}} = k_\alpha(k)(\alpha_d - \overline{\alpha}), t \in [a_k, \tau_{k+1}]$$

The solution of above ODE leads to equation (14). ■

The following lemma provides a sufficient condition under which sequence $\{\bar{U}_k\}_{k=0}^{\infty}$ is a supermartingale. The supermartingale property is later used to prove that $\alpha(t)$ is almost-surely convergent.

Lemma 4.4: Consider the system in (6-8) and suppose the number of bits R_k received over time interval $[\tau_k, a_k)$ satisfies the probability bound (5). Let

$$G(\alpha, L) = e^{-h(\alpha,L)\gamma(\alpha,L)}(1 + h(\alpha, L)\gamma(\alpha, L))$$

be non-negative, monotone increasing function with respect to α and L, respectively. If

$$G(\alpha(\tau_k), L(\tau_k)) \leq \eta \Lambda_{k-1}(k_L)^{-1}, \forall k \in \mathbb{Z}_+ \tag{19}$$

then for any $\eta \in (0, 1]$,

$$\mathbb{E}(\bar{U}_k | \bar{U}_{k-1}) \leq \eta \bar{U}_{k-1}, \forall k \in \mathbb{Z}_+ \tag{20}$$

Proof: The proof is identical to Lemma 4.4 in [8], and is omitted here for space. ■

Remark 4.5: Inequality (19) can be interpreted as a partition of the system state space with respect to the performance specification η. The parameter $\underline{\eta}$ may be viewed as the convergence rate for sequence $\{\bar{U}_k\}_{k=0}^{\infty}$. It provides a way to relate the channel state to the physical state.

The following lemma provides a sufficient condition for selecting a controller pair (k_α, k_L) that enforces the above Lemma 4.4.

Lemma 4.6: Consider the closed-loop system in equations (6-8). Suppose the wireless channel the *EBB* model (5). Given the function G in Lemma 22, if there exists a sequence of controller gains $\{(k_\alpha(k), k_L(k))\}_{k=0}^{\infty}, (k_\alpha(k), k_L(k)) \in \mathscr{K}, k \in \mathbb{Z}$ such that for $\eta \in (0, 1)$,

$$\begin{aligned} \tilde{G}(k_\alpha(k), k_L(k))\Lambda_k(k_L(k-1), k_L(k)) &\leq \eta \qquad (21) \\ \tilde{G}(k_\alpha(k), k_L(k)) &= G(\underline{\alpha}_{k+1}, \underline{L}_{k+1}) \end{aligned}$$

$$\begin{aligned} \underline{\alpha}_{k+1} &= (\hat{\alpha}(a_k) - \alpha_d)e^{-k_\alpha(k)(T-\Delta)} + \alpha_d + \Lambda_k(k_L(k))\bar{U}_k \\ \underline{L}_{k+1} &= [L(a_k) - (L_d + \frac{2v_1}{k_L(k)})]e^{-k_L(k)(T-\Delta)} + L_d + \frac{2v_1}{k_L(k)} \end{aligned}$$

Then, the following supermartingale property for $\{\bar{U}_k\}_{k=0}^{\infty}$ holds, i.e.

$$\mathbb{E}(\bar{U}_{k+1} | \bar{U}_k) \leq \eta \bar{U}_k, \forall k \in \mathbb{Z}_+ \tag{22}$$

Proof: From Lemma 4.4, we know that one sufficient condition to ensure (22) is

$$G(\alpha(\tau_{k+1}), L(\tau_{k+1})) \leq \eta \Lambda_k(k_L(k-1), k_L(k))^{-1}, \forall k \in \mathbb{Z}$$

Since

$$|e^-(\tau_{k+1})| = |\alpha(\tau_{k+1}) - \hat{\alpha}(\tau_{k+1})| \leq \Lambda_k(k_L(k-1), k_L(k))\bar{U}_k,$$

we have

$$\alpha(\tau_{k+1}) \leq \hat{\alpha}(\tau_{k+1}) + \Lambda_k(k_L(k-1), k_L(k))\bar{U}_k$$

Because $\hat{\alpha}(\tau_{k+1}) = (\hat{\alpha}(a_k) - \alpha_d)e^{-k_\alpha(k)(T-\Delta)} + \alpha_d$, then

$$\begin{aligned} \alpha(\tau_{k+1}) &\leq (\hat{\alpha}(a_k) - \alpha_d)e^{-k_\alpha(k)(T-\Delta)} + \alpha_d \\ &\quad + \Lambda_k(k_L(k-1), k_L(k))\bar{U}_k \doteq \underline{\alpha}_{k+1} \end{aligned} \tag{23}$$

From inequality (11), we obtain

$$\begin{aligned} L(\tau_{k+1}) &\leq \left[L(a_k) - (L_d + \frac{2v_1}{k_L(k)})\right] e^{-k_L(k)(T-\Delta)} \\ &\quad + L_d + \frac{2v_1}{k_L(k)} \doteq \underline{L}_{k+1} \end{aligned} \tag{24}$$

Moreover, given the fact that $G(\alpha(\tau_{k+1}), L(\tau_{k+1}))$ is a non-negative monotone increasing function with respect to α and L, then combining inequalities (23) and (24) leads to

$$G(\alpha(\tau_{k+1}), L(\tau_{k+1})) \leq G(\underline{\alpha}_{k+1}, \underline{L}_{k+1})$$

Therefore, the inequality condition (21) on the selection of controller gain assures supermartingle property (22) for sequence $\{\bar{U}_k\}_{k=0}^{\infty}$. ■

Remark 4.7: At time instant $a_k, \forall k \geq 0$, one controller pair $(k_\alpha(k), k_L(k))$ is selected based on condition (21). There might exist more than one controller pairs satisfying condition (21). We could select the pair that minimizes $\underline{\eta}$.

The following corollary proves that the sequence $\{\bar{U}_k\}_{k=0}^{\infty}$ is almost-surely convergent when Lemma 4.6 holds.

Corollary 4.8: Suppose sequence $\{\bar{U}_k\}_{k=0}^{\infty}$ is generated by equation (13), if there exists a sequence of controller pair $\{(k_\alpha(k), k_L(k))\}_{k=0}^{\infty}$ such that equation (22) holds for all $k \geq 0$, then the sequence $\{\bar{U}_k\}_{k=0}^{\infty}$ is almost-surely convergent to zero.

Proof: Since $\mathbb{E}(\bar{U}_{k+1} | \bar{U}_k) \leq \eta \bar{U}_k, \forall k \in \mathbb{Z}$ holds, this also implies

$$\mathbb{E}(\bar{U}_k) \leq \eta \mathbb{E}(\bar{U}_{k-1}) \leq \ldots \leq \eta^k \bar{U}_0$$

Let $k \to \infty$, the limit yields

$$\limsup_{k \uparrow \infty} \mathbb{E}[\bar{U}_k] \leq \lim_{k \uparrow \infty} \delta^k \bar{U}_0 = 0$$

We can then use the Markov property to show that $\{\bar{U}_k\}_{k=0}^{\infty}$ is almost-surely convergent to zero. ■

With Corollary 4.8, the following theorem proves almost-sure asymptotic stability for the α-system in equation (7).

Theorem 4.9: Consider the closed-loop system in equations (6-8). If there exists a sequence of controller pair $\{k_\alpha(k), k_L(k)\}_{k=0}^{\infty}$ such that Lemma 4.4 holds, then the random process $\{\alpha(t) : t \in \mathbb{R}_+\}$ is almost-surely convergent to α_d.

Proof: Without loss of generality, we let $\alpha_d = 0$. Consider $t \in [\tau_k, \tau_{k+1})$, we have

$$\hat{\alpha}^-(\tau_{k+1}) = e^{-k_\alpha(k)(T-\Delta)} e^{-k_\alpha(k-1)\Delta} \hat{\alpha}(\tau_k)$$

Let $E(\tau_{k+1}) := \hat{\alpha}(\tau_{k+1}) - \hat{\alpha}^-(\tau_{k+1})$, then

$$\hat{\alpha}(\tau_{k+1}) = e^{-k_\alpha(k)(T-\Delta)} e^{-k_\alpha(k-1)\Delta} \hat{\alpha}(\tau_k) + E(\tau_{k+1})$$

Let $k_\alpha^* = \min\{k_\alpha | k_\alpha \in \mathscr{K}\}$,

$$|\hat{\alpha}(\tau_{k+1})| \leq e^{-k_\alpha^* T} |\hat{\alpha}(\tau_k)| + |E(\tau_{k+1})| \tag{25}$$

The term $|E(\tau_{k+1})|$ can be further bounded by

$$\begin{aligned} |E(\tau_{k+1})| &\leq \Lambda_k(k_L(k-1),k_L(k))\bar{U_k}(1-2^{-R_{k+1}}) \\ &\leq \Lambda_k(k_L(k-1),k_L(k))\bar{U_k} \end{aligned} \quad (26)$$

Similarly, let

$$\Lambda^* = \max\{\Lambda_k(k_L(k-1),k_L(k))|k_L(k-1),k_L(k) \in \mathscr{K}\},$$

then inequality (26) may be further bounded as $|E(\tau_{k+1})| \leq \Lambda^*\bar{U_k}$. Taking the expectation on both sides of inequalities (25) and using the above bound on $|E(\tau_{k+1})|$ yields

$$\mathbb{E}(|\hat{\alpha}(\tau_{k+1})|) \leq e^{-k_\alpha^* T}\mathbb{E}(|\hat{\alpha}(\tau_k)|) + \Lambda^*\mathbb{E}(\bar{U_k})$$

With the result from Corollary 4.8, we have

$$\begin{aligned} \mathbb{E}(|\hat{\alpha}(\tau_{k+1})|) &\leq e^{-k_\alpha^* T(k+1)}\mathbb{E}(|\hat{\alpha}(0)|) \\ &\quad + \bar{U}_0\Lambda^*\eta^k\sum_{i=0}^{k}(\frac{e^{-k_\alpha^* T}}{\eta})^i \\ &\leq e^{-k_\alpha^* T(k+1)}\mathbb{E}(|\hat{\alpha}(0)|) \\ &\quad + \frac{\eta^{k+1}-e^{-k_\alpha^* T(k+1)}}{\eta - e^{-k_\alpha^* T}}\bar{U}_0\Lambda^* \end{aligned}$$

Here, it is straightforward to see that

$$\lim_{k\to\infty}\mathbb{E}(|\hat{\alpha}(\tau_k)|) \to 0$$

With the result from Corollary 4.8, i.e. $\lim_{k\to\infty}\mathbb{E}(|\bar{U_k}|) \to 0$, we have

$$\begin{aligned} \lim_{k\to\infty}\mathbb{E}(|\alpha(\tau_k)|) &\leq \lim_{k\to\infty}\mathbb{E}(|\hat{\alpha}(\tau_k)| + |\bar{U_k}|) \\ &= \lim_{k\to\infty}\mathbb{E}(|\hat{\alpha}(\tau_k)|) + \lim_{k\to\infty}\mathbb{E}(|\bar{U_k}|) \to 0 \end{aligned}$$

As noted before, one can then use the Markov inequality to verify almost-sure convergence of the sequence $\{|\alpha(\tau_k)|\}$ to zero. We also know, however, that the time between successive sampling instants is a constant and that the system trajectory is uniformly bounded between these instants (due to the Lipschitz assumption). We can therefore conclude that all sample paths of the continuous-time signal $\alpha(t)$ must be almost-surely convergent to 0. ■

V. Simulation Results

This section presents simulation experiments examining the resilience of our proposed switched controller's to deep fades.

A two-state Markov chain model was used to simulate the fading channel between the leader and follower. One state represents the good channel condition, which simply means the transmitted bit is successfully received. The other state is the bad channel condition, which represents the failure of receiving the bit. The conditional probabilities of remaining in the good or bad channel state are $p_{11} = e^{-3\times10^{-3}(\frac{L(t)}{\cos\alpha(t)})^2}$ and $p_{22} = e^{-6\times10^2(\frac{\cos\alpha(t)}{L(t)})^2}$, respectively. The corresponding transition probabilities between these states are $1-p_{11}$ and $1-p_{22}$. The EBB model for this channel has the parameters

$$h(\alpha,L) = \bar{R}e^{-3\times10^{-4}(\frac{L(t)}{\cos\alpha(t)})^2}, \gamma(\alpha,L) = e^{-4.5\times10^{-3}(\frac{L(t)}{\cos\alpha(t)})^2}$$

The other simulation parameters are

$$T = 0.1, \Delta = 0.02, \bar{R} = 2;$$
$$v_1 = 20, L_d = 5, \alpha_d = \frac{\pi}{3}, d = 1.$$

The regulation law $g(\cdot)$ for the leader's heading angle is assumed to be a linear function $g(\alpha) = 2\alpha$. The initial inter-vehicle distance is $L(0) = 80$ and the initial bearing angle is $\alpha(0) = \pi/12$. The initial bearing estimate is $\hat{\alpha}(0) = 0$ with the $U_0 = \pi/12$. The selection pool for the controller pair is

$$\mathscr{K} = \left\{(k_L,k_\alpha) : \frac{2v_1}{L_d - d} \leq k_L \leq 100, 5 \leq k_\alpha \leq 100\right\}.$$

A Monte Carlo method was used to verify that the system had almost-sure asymptotic stability when Lemma 4.4 holds. In the simulation, we selected the controller pair from $\mathscr{K}$ that minimizes η at each time instance a_k. The simulation was run 100 times over the time interval from 0 to 2 seconds. Figure 2 shows the maximum and minimum value of the system state α and L with the switching policy over all the 100 runs. The top plot in the figure is the trajectory for state α, with maximum value marked as blue solid line, and minimum value as red dashed-dot line. The two dashed lines represent the upper and lower bound for the relative bearing α, i.e. $|\alpha| \leq \pi/2$. The bottom plot is the trajectory for the relative distance L with the same marking rule. We can see from the plots that the maximum and minimum values of the system state converge to the desired set-point $\alpha_d = \frac{\pi}{2}$ and $L_d = 5$ asymptotically. These results are consistent with our statements in Lemma 4.6 for almost-sure asymptotic stability.

We also studied the benefits of such a switching policy over a non-switching strategy. For a fair comparison, we selected two types of controllers as representatives of the non-switching strategy, which are $(20,20)$ and $(100,100)$. The pair $(20,20)$ represents the small-gain controller, while $(100,100)$ is the high-gain controller. We ran the simulation for 2 seconds over 100 runs with the same simulation parameters. Figure 3 shows the maximum and minimum value for the state trajectory with the small-gain controller $(20,20)$, while Figure 4 is for the high-gain controller $(100,100)$. The system trajectories also asymptotically converge to the set-points for both cases. This is not surprising since the result in Lemma 4.6 are only a sufficient condition. However, as is shown in these figures, the relative bearing angles α generated by either controller fail to satisfy the bound $|\alpha| \leq \frac{\pi}{2}$. This bound is important due to the directional nature of the antenna. When $|\alpha| > \frac{\pi}{2}$, the antenna will have no gain in that direction and hence the communication link between leader and follower will be broken. On the other hand, the switching strategy generated a smoother trajectory with smaller variance. More importantly, Figure 2 clearly shows that the bearing angle constraint was always satisfied.

One sample path of the switching profile is shown in Figure 5. The bottom plot is the channel state (R_k) along the time line. The top plot is the switching profile that reacts to the change of R_k. As shown in the figure, the controller k_L switches from lower gain to the high gain

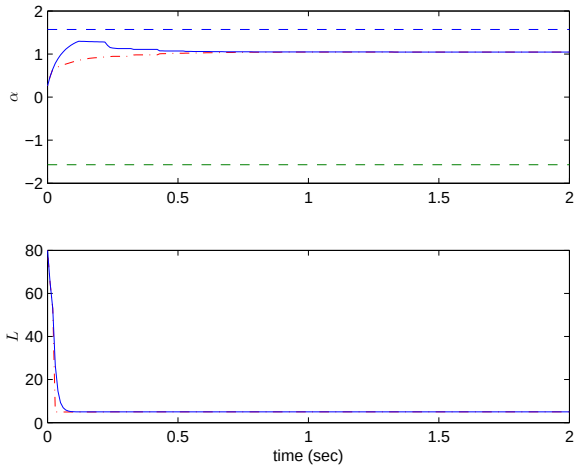

Fig. 2. Almost-sure asymptotic stability with switching strategy

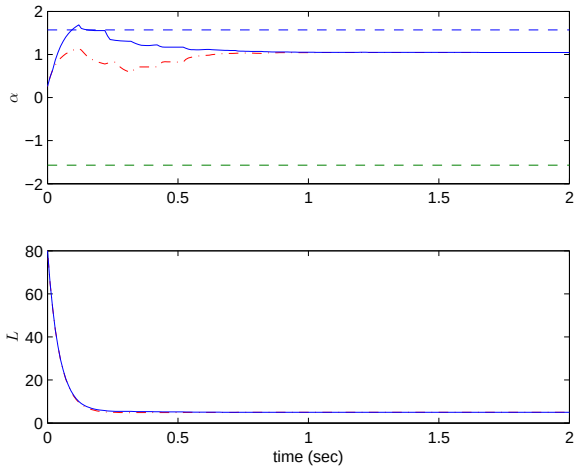

Fig. 3. The maximum and minimum system trajectory with non-switching controller $k_L = 20$ and $k_\alpha = 20$

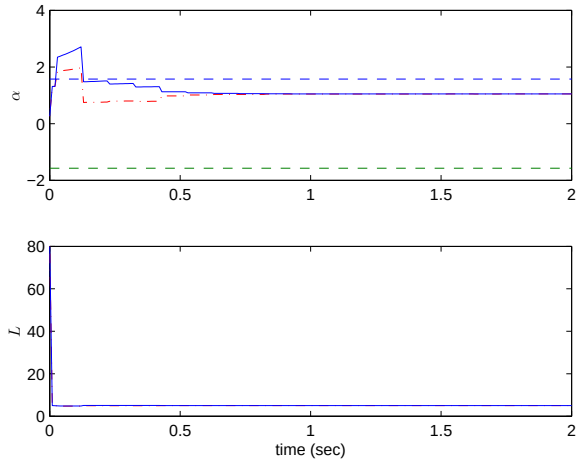

Fig. 4. The maximum and minimum system trajectory with non-switching controller $k_L = 100$ and $k_\alpha = 100$

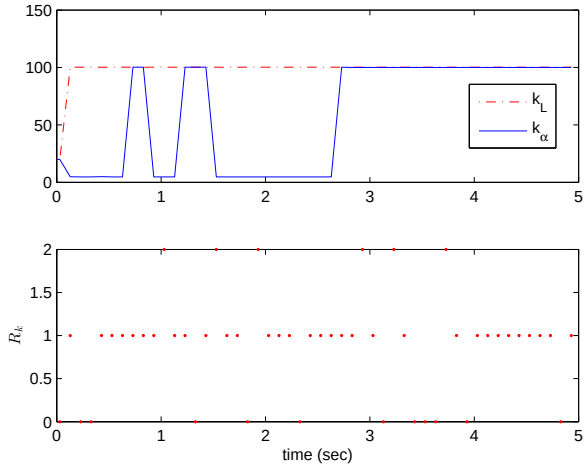

Fig. 5. One sample of the switching profile and channel state (R_k)

after 0.2 seconds when the system state is close enough to the desired set-point. The controller k_α exhibits different switching behaviors. It first selects the low gain controller because of the low channel state, and then switches back and forth in response to changes in the channel state. After the system state reaches the set-point, k_α stays high all the time.

The channel state profile in Figure 5 represents just one possible sample path. It is possible (though unlikely) for the channel to generate a "string" of dropouts. We're interested in seeing how well our switched controller performs even under such low probability events. A simulation run was therefore done in which the communication link was broken for $N = 10$ consecutive transmissions, starting 1 second into the simulation. We refer to this sequence of dropouts as a "fault". The simulation was again run 100 times from 0 second to 10 second with the same parameters. Figure 6 shows the response of the system state in terms of maximum and minimum value with the switching control strategy. At time interval $[0,1]$, the system is steering to the set-point without fault. The fault occurs at around 1 second, and drives the system out of the antenna's radiation range. The system detects this fault, and switches the controller to drive the system back to the set-point after around 2 second.

For comparison purposes, we also simulated faulty system using two control strategies that used no channel state information to combat the fault. The first strategy employs the non-switching safe controller $(20,20)$. The second strategy uses only system state information to switch the controller between small gain $(20,20)$ and high gain $(100,100)$. This was done when the system uncertainty $|\alpha - \hat{\alpha}|$ exceeded a specified threshold θ_0. Neither of these controllers was able to stabilize the system in the presence of the fault. A sample path for the system under the second controller is shown in Figure 7.

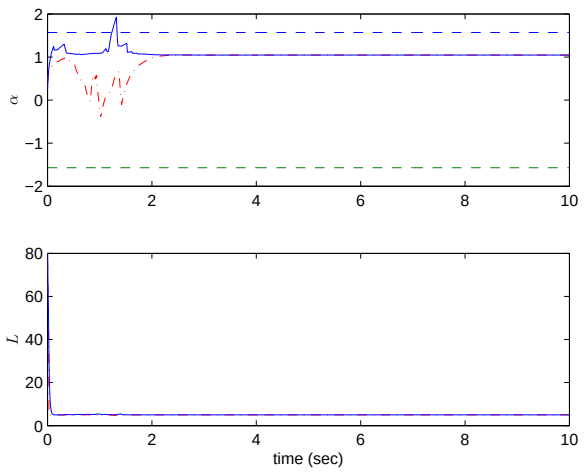

Fig. 6. System response to unexpected fault using switching strategy

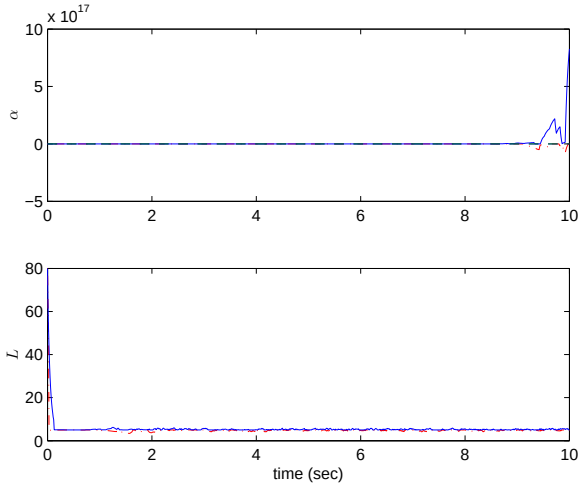

Fig. 7. System response to unexpected fault using state-based switching strategy with threshold $\frac{\pi}{6}$

VI. Conclusion

This paper studied the almost-sure stability for leader-follower formation control of nonholomonic systems in the presence of deep fades exhibiting exponentially bounded burstiness. The paper establishes sufficient conditions to switch the controller to assure almost-sure asymptotic stability. Preliminary simulation results support the analysis' conclusions. Future work will extend these concepts from leader-follower formations to more general formation control problems.

References

[1] C. A. Balanis. *Antenna theory: analysis and design/Constantine A. Balanis*. J. Wiley, New York, 1982.

[2] T. Balch and R. C. Arkin. Behavior-based formation control for multirobot teams. *Robotics and Automation, IEEE Transactions on*, 14(6):926–939, 1998.

[3] R. W. Brockett and D. Liberzon. Quantized feedback stabilization of linear systems. *Automatic Control, IEEE Transactions on*, 45(7):1279–1289, 2000.

[4] L. Cheng, B. E. Henty, D. D. Stancil, F. Bai, and P. Mudalige. Mobile vehicle-to-vehicle narrow-band channel measurement and characterization of the 5.9 ghz dedicated short range communication (dsrc) frequency band. *IEEE Journal on Selected Areas in Communications*, 25(8):1501–1516, 2007.

[5] J. P. Desai, J. Ostrowski, and V. Kumar. Controlling formations of multiple mobile robots. In *Robotics and Automation, 1998. Proceedings. 1998 IEEE International Conference on*, volume 4, pages 2864–2869. IEEE, 1998.

[6] N. Elia and S. K. Mitter. Stabilization of linear systems with limited information. *IEEE Transactions on Automatic Control*, 46(9):1384–1400, 2001.

[7] J. P. Hespanha, D. Liberzon, and A. S. Morse. Towards the supervisory control of uncertain nonholonomic systems. In *American Control Conference, 1999. Proceedings of the 1999*, volume 5, pages 3520–3524. IEEE, 1999.

[8] B. Hu and M. D. Lemmon. Using channel state feedback to achieve resilience to deep fades in wireless networked control systems. In *Proceedings of the 2nd international conference on High Confidence Networked Systems*, April 9-11 2013.

[9] H. Kushner. *Stochastic Stability and Control*. Academic Press, 1967.

[10] N. C. Martins, M. A. Dahleh, and N. Elia. Feedback stabilization of uncertain systems in the presence of a direct link. *IEEE Transactions on Automatic Control*, 51(3):438–447, 2006.

[11] M. Mesbahi and M. Egerstedt. *Graph theoretic methods in multiagent networks*. Princeton University Press, 2010.

[12] P. Minero, M. Franceschetti, S. Dey, and G. N. Nair. Data rate theorem for stabilization over time-varying feedback channels. *IEEE Transactions on Automatic Control*, 54(2):243–255, 2009.

[13] N. Moshtagh and A. Jadbabaie. Distributed geodesic control laws for flocking of nonholonomic agents. *Automatic Control, IEEE Transactions on*, 52(4):681–686, 2007.

[14] R. Olfati-Saber, J. A. Fax, and R. M. Murray. Consensus and cooperation in networked multi-agent systems. *Proceedings of the IEEE*, 95(1):215–233, 2007.

[15] D. J. Stilwell and B. E. Bishop. Platoons of underwater vehicles. *Control Systems, IEEE*, 20(6):45–52, 2000.

[16] D. M. Stipanović, G. I?nalhan, R. Teo, and C. J. Tomlin. Decentralized overlapping control of a formation of unmanned aerial vehicles. *Automatica*, 40(8):1285–1296, 2004.

[17] S. Tatikonda and S. Mitter. Control under communication constraints. *IEEE Transactions on Automatic Control*, 49(7):1056–1068, 2004.

[18] D. Tse and P. Viswanath. *Fundamentals of wireless communication*. Cambridge university press, 2005.

[19] P. Varaiya. Smart cars on smart roads: problems of control. *Automatic Control, IEEE Transactions on*, 38(2):195–207, 1993.

[20] H. Wang and N. Moayeri. Finite-state markov channel - a useful model for radio communication channels. *IEEE Transactions on Vehicular Technology*, 44(1):163–171, 1995.

[21] W. S. Wong and R. W. Brockett. Systems with finite communication bandwidth constraints. ii. stabilization with limited information feedback. *IEEE Transactions on Automatic Control*, 44(5):1049–1053, 1999.

[22] O. Yaron and M. Sidi. Performance and stability of communication networks via robust exponential bounds. *IEEE/ACM Transactions on Networking*, 1(3):372–385, 1993.

[23] S. Yi, Y. Pei, and S. Kalyanaraman. On the capacity improvement of ad hoc wireless networks using directional antennas. In *International Symposium on Mobile Ad Hoc Networking & Computing: Proceedings of the 4 th ACM international symposium on Mobile ad hoc networking & computing*, volume 1, pages 108–116. Citeseer, 2003.